Contribution from the Department of Chemistry, West Virginia University, Morgantown, West Virginia 26506, and the School of Chemical Sciences, University of Illinois, Urbana, Illinois 61801

Crystal and Molecular Structure of Di-μ-azido-bis(2,2',2''-triaminotriethylamine)dinickel(II) Tetraphenylborate. Magnetic Exchange between Azide-Bridged Octahedral Nickel(II) Centers—the Di-μ-azido and Mono-μ-azido Cases

CORTLANDT G. PIERPONT,[1*] DAVID N. HENDRICKSON,*[2,3] D. MICHAEL DUGGAN,[2] FRANK WAGNER,[2] and E. KENT BAREFIELD[2]

Received June 3, 1974 AIC40353L

The structure of $[Ni_2(tren)_2(N_3)_2](BPh_4)_2$, where tren is 2,2',2''-triaminotriethylamine, has been determined using heavy-atom least-squares X-ray methods giving conventional discrepancy factors of $R_F = 0.048$ and $R_{wF} = 0.050$ for 1982 reflections measured on a four-circle automated diffractometer. The compound crystallizes in the $P2_1/a$ space group with two formula weights in a cell measuring $a = 16.508$ (3) Å, $b = 19.658$ (3) Å, $c = 10.431$ (3) Å, and $\beta = 121.69$ (5)°. The crystal densities are 1.304 g/cm^3 (calculated) and 1.29 (1) g/cm^3 (measured). Discrete cationic $[Ni_2(tren)_2(N_3)_2]^{2+}$ and anionic BPh_4^- units are found. Two linear groups are bridging the nickel(II) atoms in an end-to-end fashion. The two azide groups are parallel and the nickel atoms are found above and below the azide plane by 0.52 Å. Each azide bridge is asymmetric with Ni–N–N angles of 135.3 (7) and 123.3 (6)° and Ni–N distances of 2.069 (8) and 2.195 (7) Å. The coordination geometry at each nickel atom is approximately octahedral. The previously reported magnetic properties of $[Ni_2(tren)_2(N_3)_2](BPh_4)_2$ (the exchange parameter $J = -35$ cm^{-1}) are compared with those measured in this work for the *single* end-to-end azide-bridged $[Ni_2(macro)_2(N_3)_3]I$, where macro is 1,4,8,11-tetramethyl-1,4,8,11-tetraazacyclotetradecane. In this latter case there is a weaker antiferromagnetic interaction with $J = -12.3$ cm^{-1}. The difference in magnetic interaction in these two end-to-end azide-bridged compounds is qualitatively discussed in terms of bonding differences.

Introduction

The structural characteristics and chemistry of coordinated azides have very recently been reviewed.[4] X-Ray structures have been reported for some ten transition metal complexes having an azide group bound to one metal atom and for two complexes with an azide group bridging two metal atoms through the same nitrogen. At the time of the review there was only one complex known that possessed an azide group bridging two metal atoms through the two end nitrogens (*i.e.*, 1,3-μ-azido). This complex is $[Cu(P(C_6H_5)_3)_2N_3]_2$.[5]

Very recently we reported[6] the synthesis and characterization of di-μ-azido-bis(2,2',2''-triaminotriethylamine)dinickel(II) tetraphenylborate, $[Ni_2(tren)_2(N_3)_2](BPh_4)_2$. The dimeric nature of the cation was deduced from a variable-temperature magnetic susceptibility determination. A comparison of the X-ray powder pattern with that for the oxalate-bridged analog and an analysis of the infrared spectrum, which indicated little intensity in the symmetric azide stretch, pointed to the presence of end-to-end, that is, di-μ(1,3)-azido bridging in the compound. In this paper we report the molecular structure of $[Ni_2(tren)_2(N_3)_2](BPh_4)_2$ as determined by X-ray methods. The magnetic exchange properties of this compound are compared with data obtained for $[Ni_2(macro)_2(N_3)_3]I$, where macro is 1,4,8,11-tetramethyl-1,4,8,11-tetraazacyclotetradecane. The latter compound has been shown[7] to possess a *single* 1,3-azido bridge.

Experimental Section

Compound Preparation and Magnetic Susceptibility Determination. Samples of the compounds $[Ni_2(tren)_2(N_3)_2](BPh_4)_2$ and $[Ni_2(macro)_2(N_3)_3]I$ were prepared as previously reported[6,7] and analyses in our school of Chemical Sciences microanalytical laboratory showed them to be pure. The variable-temperature magnetic susceptibility of $[Ni_2(macro)_2(N_3)_3]I$ was determined using a PAR Model 150A magnetometer employing a $CuSO_4 \cdot 5H_2O$ standard and a 14.8-kG field. Details of the susceptibility experiment as well as comments on the theoretical equations and least-squares fitting procedure can be gleaned from an earlier paper.[8]

X-Ray Crystal Measurements. A crystal of the complex $[Ni_2(tren)_2(N_3)_2](BPh_4)_2$ of dimensions 0.192 × 0.210 × 0.213 mm was observed to have approximate $2/m$ symmetry and was mounted along the twofold axis. Precession and Weissenberg photographs taken on the crystal indicated the monoclinic system with observed extinctions of $0k0$, $k = 2n + 1$, and $h0l$, $h = 2n + 1$, consistent with space group $P2_1/a$. The lattice constants were determined at ambient room temperature from a least-squares refinement of the angular settings of 18 strong, independent reflections centered on a Picker four-circle automated diffractometer using Mo Kα radiation (λ 0.7107 Å) and are $a = 16.508$ (3) Å, $b = 19.658$ (3) Å, $c = 10.431$ (3) Å, $\beta = 121.69$ (5)°, and $V = 2880$ Å^3. An experimental density of 1.29 (1) g/cm^3 agrees with a calculated density of 1.304 g/cm^3 for two dimeric formula weights per unit cell. Thus, a crystallographic center of inversion is imposed on the cationic complex. The mosaic spread of the crystal was determined using the narrow-source open-counter ω-scan technique.[9] The average width at half-height was acceptable at 0.08°. An independent set of intensity data was collected by the θ–2θ scan technique using the Zr-filtered Mo Kα peak with allowances made for the $K_{\alpha 1}$–$K_{\alpha 2}$ separation at higher 2θ values. The data set was collected within the angular range $4.5 \leq 2\theta \leq 48°$. Attenuators were inserted automatically if the count rate of the diffracted beam exceeded 9000 counts/sec during the scan. The attenuators used were brass foil of thickness chosen to give an approximate attenuation factor of 2.5. During data collection the intensities of four standard reflections in different regions of reciprocal space were monitored after every 100 reflections measured. None of these standards deviated from its mean value by more than 3% during the time required to collect the data. Data were processed in the usual way with values of I and $\sigma(I)$ corrected for Lorentz and polarization effects. Since the crystal was approximately equidimensional and the linear absorption coefficient small ($\mu = 7.1$ cm^{-1}), no correction was made for absorption effects. The intensities of a total of 3740 reflections were measured, of which 1982 were observed to be greater than 2σ and have been included in the refinement.

Solution and Refinement of the Structure. The position of the Ni atom was determined from a three-dimensional Patterson map. Two cycles of least-squares refinement of the nickel positional and thermal parameters and a scale factor gave discrepancy indices $R_F = \sum||F_o| - |F_c||/\sum|F_o|$ and $R_{wF} = (\sum w(|F_o| - |F_c|)^2/\sum wF_o^2)^{1/2}$ of 0.485 and 0.513, respectively. From the Fourier map based on this refinement the positions of all nonhydrogen atoms of the structure were obtained. Isotropic refinement of all atoms with phenyl rings of the anion treated as rigid groups (d(C–C) = 1.392 Å) with a single-group thermal parameter converged to discrepancy indices of $R_F = 0.091$ and $R_{wF} = 0.101$. Further refinement with anisotropic thermal parameters for nongroup atoms and individual isotropic thermal parameters for atoms of the groups converged to $R_F = 0.058$ and $R_{wF} = 0.062$. The positions of the 18 hydrogen atoms of the tren ligand were then determined from a Fourier map and refined with isotropic thermal parameters in a final cycle of least squares including fixed contributions

Table I. Final Positional, Thermal, and Group Parameters for $[Ni_2(tren)_2(N_3)_2](B(C_6H_5)_4)_2$

Atom[a]	x	y	z	β_{11}[b]	β_{22}	β_{33}	β_{12}	β_{13}	β_{23}
Ni	0.12399 (7)	0.09036 (4)	0.02732 (9)	0.00545 (8)	0.00246 (3)	0.01204 (15)	−0.00072 (4)	0.00469 (8)	−0.00075 (5)
N(1)	0.0107 (6)	0.0898 (3)	0.0599 (7)	0.0093 (7)	0.0031 (3)	0.0236 (12)	−0.0016 (3)	0.0099 (7)	−0.0014 (4)
N(2)	−0.0341 (5)	0.0476 (4)	0.0743 (6)	0.0054 (7)	0.0033 (3)	0.0142 (10)	−0.0002 (3)	0.0054 (6)	−0.0019 (4)
N(3)	−0.0797 (6)	0.0073 (4)	0.0924 (7)	0.0102 (7)	0.0038 (3)	0.0218 (12)	−0.0021 (3)	0.0106 (8)	−0.0028 (4)
N(4)	0.2338 (4)	0.1071 (3)	−0.0111 (6)	0.0049 (5)	0.0029 (2)	0.0124 (9)	−0.0003 (2)	0.0034 (5)	−0.0002 (3)
N(5)	0.2268 (5)	0.0364 (3)	0.2140 (6)	0.0092 (6)	0.0026 (2)	0.0149 (10)	−0.0003 (3)	0.0072 (6)	0.0003 (3)
N(6)	0.1667 (4)	0.1831 (3)	0.1365 (6)	0.0053 (5)	0.0026 (2)	0.0190 (11)	0.0001 (2)	0.0053 (6)	−0.0007 (3)
N(7)	0.0430 (5)	0.1306 (3)	−0.1935 (7)	0.0060 (6)	0.0051 (3)	0.0169 (11)	0.0003 (3)	0.0042 (6)	0.0012 (4)
C(1)	0.3111 (6)	0.0547 (4)	0.0822 (9)	0.0092 (8)	0.0035 (3)	0.0172 (14)	0.0018 (4)	0.0069 (9)	0.0020 (5)
C(2)	0.3202 (7)	0.0520 (4)	0.2335 (8)	0.0062 (7)	0.0033 (3)	0.0144 (13)	0.0009 (3)	0.0038 (8)	0.0016 (4)
C(3)	0.2710 (6)	0.1790 (4)	0.0375 (8)	0.0063 (7)	0.0031 (3)	0.0193 (14)	−0.0011 (3)	0.0054 (8)	0.0004 (5)
C(4)	0.2012 (6)	0.2239 (4)	0.0549 (9)	0.0075 (8)	0.0021 (3)	0.0257 (16)	−0.0014 (3)	0.0078 (9)	−0.0022 (5)
C(5)	0.1916 (6)	0.0973 (4)	−0.1757 (8)	0.0062 (7)	0.0051 (3)	0.0104 (11)	−0.0001 (4)	0.0048 (7)	−0.0004 (5)
C(6)	0.1025 (7)	0.1404 (4)	−0.2603 (8)	0.0083 (9)	0.0068 (4)	0.0107 (12)	0.0001 (4)	0.0052 (9)	0.0019 (5)
B	0.2174 (6)	0.3953 (4)	0.4186 (8)	0.0030 (6)	0.0030 (3)	0.0112 (12)	0.0000 (3)	0.0024 (6)	0.0000 (4)

Group[c]	x_c	y_c	z_c	ϕ	θ	ρ
R(1)	0.0457 (2)	0.3549 (1)	0.1089 (3)	−0.130 (3)	2.556 (3)	−2.351 (3)
R(2)	0.1878 (2)	0.3704 (1)	0.6817 (3)	−1.751 (3)	−3.039 (3)	1.456 (2)
R(3)	0.2655 (2)	0.5474 (2)	0.4692 (3)	−1.785 (3)	3.068 (3)	3.055 (2)
R(4)	0.3683 (2)	0.3115 (1)	0.4022 (3)	−0.026 (4)	2.345 (3)	−0.820 (4)

[a] Estimated standard deviations of the least significant figures are given in parentheses here and in succeeding tables. [b] Anisotropic thermal parameters are in the form $\exp[-(h^2\beta_{11} + k^2\beta_{22} + l^2\beta_{33} + 2hk\beta_{12} + 2hl\beta_{13} + 2kl\beta_{23})]$. [c] x_c, y_c, and z_c are the fractional coordinates of the rigid-group centers. The angles ϕ, θ, and ρ are in radians and have been previously defined by R. Eisenberg and J. A. Ibers, *Inorg. Chem.*, 4, 773 (1965).

Table II. Refined Hydrogen Atom Positions in $[Ni_2(tren)_2(N_3)_2](B(C_6H_5)_4)_2$

Atom	x	y	z	B, Å^2
N5H(1)	0.236 (6)	0.046 (4)	0.313 (9)	5.0 (7)
N5H(2)	0.225 (5)	−0.011 (4)	0.212 (7)	3.2 (6)
C1H(1)	0.278 (7)	0.010 (5)	0.021 (9)	8.2 (9)
C1H(2)	0.318 (6)	0.078 (4)	0.051 (9)	5.6 (7)
C2H(1)	0.359 (5)	0.019 (3)	0.287 (7)	2.4 (6)
C2H(2)	0.357 (5)	0.094 (3)	0.296 (7)	2.6 (6)
N6H(1)	0.107 (5)	0.219 (3)	0.122 (8)	3.7 (7)
N6H(2)	0.234 (7)	0.186 (5)	0.254 (10)	10.2 (12)
C3H(1)	0.342 (6)	0.169 (4)	0.169 (9)	4.3 (7)
C3H(2)	0.284 (7)	0.186 (5)	−0.072 (10)	9.4 (10)
C4H(1)	0.234 (4)	0.262 (3)	0.123 (6)	1.1 (6)
C4H(2)	0.125 (7)	0.238 (4)	−0.042 (9)	8.2 (9)
N7H(1)	0.005 (4)	0.160 (3)	−0.231 (6)	1.5 (6)
N7H(2)	0.002 (6)	0.094 (4)	−0.248 (8)	4.4 (7)
C5H(1)	0.255 (6)	0.110 (3)	−0.186 (8)	3.4 (6)
C5H(2)	0.187 (5)	0.042 (4)	−0.190 (8)	3.9 (6)
C6H(1)	0.112 (7)	0.182 (5)	−0.255 (10)	8.7 (8)
C6H(2)	0.065 (6)	0.126 (4)	−0.371 (10)	6.3 (7)

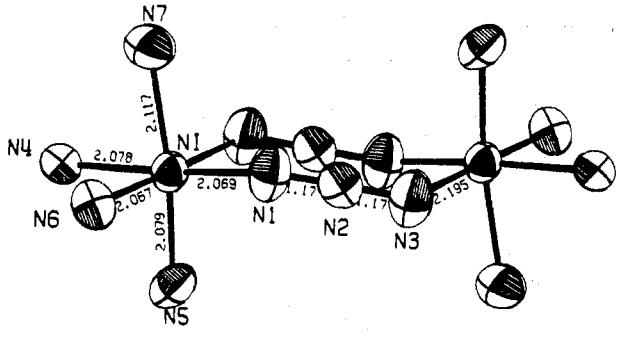

Figure 1. ORTEP plotting of $[Ni_2(tren)_2(N_3)_2]^{2+}$ showing some of the geometrical parameters; the dimer is located on a center of inversion, and carbon and hydrogen atoms are not shown.

for phenyl hydrogens (d(C–H) = 0.98 Å). The final discrepancy indices for the structure were R_F = 0.048 and R_{wF} = 0.050. During all cycles of refinement the function minimized was $\sum w(|F_o| - |F_c|)^2$ and the weights w were taken as $4F_o^2/\sigma^2(F_o^2)$. The standard deviations $\sigma(F^2)$ were estimated from counting statistics described previously.[10] In all calculations the atomic scattering factors for the nonhydrogen atoms were those of Cromer and Waber,[11] while the hydrogen scattering factors were taken from the tabulation of Stewart, *et al.*[12] The effects of anomalous dispersion were included in the calculated structure factors with the appropriate values of $\Delta f'$ and $\Delta f''$ for the Ni atom taken from the report by Cromer and Liberman.[13] At the completion of the refinement the standard deviation of an observation of unit weight was 1.23. The final positional and thermal parameters of the structure are given in Table I. Positional and thermal parameters for the hydrogen atoms are given in Table II. In Table III are the derived positional and isotropic thermal parameters of the group carbon atoms. Table IV contains root-mean-square vibrational amplitudes of atoms refined anisotropically. A table of the final F_o and $|F_c|$ values for the 1982 reflections used in the refinement is available.[14]

Table III. Derived Positional and Isotropic Thermal Parameters for Group Carbon Atoms

Atom	x	y	z	B, Å^2
		R(1)		
C(1)	−0.0287 (3)	0.3338 (3)	−0.0322 (4)	5.6 (2)
C(2)	−0.0009 (4)	0.2936 (2)	0.0941 (5)	5.0 (2)
C(3)	0.0176 (3)	0.3950 (2)	−0.0177 (4)	6.0 (2)
C(4)	0.1197 (3)	0.3758 (3)	0.2494 (4)	3.4 (1)
C(5)	0.0918 (4)	0.4161 (2)	0.1230 (5)	4.4 (2)
C(6)	0.0734 (3)	0.3146 (2)	0.2349 (4)	4.1 (2)
		R(2)		
C(1)	0.1759 (4)	0.3638 (2)	0.8038 (5)	5.4 (2)
C(2)	0.0979 (3)	0.3779 (2)	0.6611 (6)	5.5 (2)
C(3)	0.2659 (3)	0.3563 (2)	0.8247 (4)	5.2 (2)
C(4)	0.2000 (3)	0.3771 (2)	0.5601 (4)	3.5 (1)
C(5)	0.2779 (2)	0.3630 (2)	0.7028 (5)	4.2 (2)
C(6)	0.1099 (3)	0.3846 (2)	0.5393 (4)	4.6 (2)
		R(3)		
C(1)	0.2872 (3)	0.6163 (2)	0.4986 (5)	4.6 (2)
C(2)	0.1927 (3)	0.5949 (2)	0.4228 (5)	4.8 (2)
C(3)	0.3599 (2)	0.5689 (2)	0.5449 (5)	4.5 (2)
C(4)	0.2439 (3)	0.4786 (2)	0.4397 (5)	3.3 (1)
C(5)	0.3383 (3)	0.5000 (2)	0.5155 (5)	3.8 (1)
C(6)	0.1711 (2)	0.5260 (2)	0.3934 (4)	4.2 (2)
		R(4)		
C(1)	0.4346 (4)	0.2732 (3)	0.3890 (6)	5.4 (2)
C(2)	0.3999 (4)	0.2495 (2)	0.4769 (6)	5.4 (2)
C(3)	0.4030 (3)	0.3352 (2)	0.3143 (4)	4.9 (2)
C(4)	0.3021 (4)	0.3498 (3)	0.4153 (6)	3.4 (1)
C(5)	0.3368 (4)	0.3735 (2)	0.3275 (6)	4.2 (2)
C(6)	0.3336 (3)	0.2878 (2)	0.4900 (4)	4.3 (2)

Discussion of the Structure

The halves of the dimeric cation $[Ni_2(tren)_2(N_3)_2]^{2+}$ are related by a crystallographic center of inversion. The geometry about the Ni atom is octahedral with the coordination po-

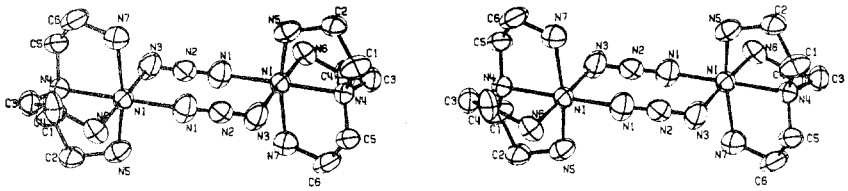

Figure 2. Stereoscopic view of $[Ni_2(tren)_2(N_3)_2]^{2+}$; hydrogen atoms are not shown.

Table IV. Root-Mean-Square Amplitudes of Vibration (Å)

Atom	Min	Intermed	Max
Ni	0.202 (2)	0.210 (2)	0.249 (1)
N(1)	0.220 (10)	0.266 (10)	0.333 (9)
N(2)	0.192 (11)	0.232 (13)	0.278 (10)
N(3)	0.235 (9)	0.238 (12)	0.355 (9)
N(4)	0.212 (8)	0.235 (8)	0.246 (8)
N(5)	0.215 (8)	0.237 (8)	0.304 (10)
N(6)	0.214 (9)	0.230 (9)	0.282 (8)
N(7)	0.238 (9)	0.277 (10)	0.321 (8)
C(1)	0.223 (11)	0.264 (11)	0.328 (12)
C(2)	0.209 (11)	0.275 (15)	0.277 (11)
C(3)	0.208 (13)	0.268 (10)	0.298 (12)
C(4)	0.178 (13)	0.273 (15)	0.328 (10)
C(5)	0.191 (11)	0.249 (14)	0.317 (10)
C(6)	0.189 (13)	0.294 (16)	0.370 (11)
B	0.174 (16)	0.226 (12)	0.241 (12)

lyhedron defined by the four nitrogen donors of the chelating, tetradentate tren ligand and the end nitrogens of centrosymmetrically related, bridging azide ligands. Perspective views of the molecule are shown in Figures 1 and 2. Intramolecular bond distances and angles are presented in Table V. There are no unusually short separations between the cationic complex and the tetraphenylborate anions.

The $Ni_2(N_3)_2$ Ring. Two particularly significant features of the nickel–azide ring are the approximate planarity of the ring and the asymmetry of the azide bridge. The Ni–N(3)' distance of 2.195 (7) Å is longer than the more regular Ni–N(1) distance of 2.069 (8) Å. Also, the Ni–N(1)–N(2) angle of 135.3 (7)° differs considerably from the more expected value of 123.3 (6)° for Ni–N(3)'–N(2)'. The center of inversion and the linearity of the N_3^- ligand (177.1 (9)°) require that the two azides be parallel. The Ni atom is located 0.52 Å (see Table VI) from the azide plane resulting in a slight pucker in the $Ni_2(N_3)_2$ ring with a dihedral angle of 20.7 (4)° between the Ni–N(1)–N(3)' plane and the azide plane. Perhaps the best illustration of the deviation of the nickel–azide ring from a more likely geometry is the dihedral angle between the two planes defined by the nickel atoms and one azide bridge. With the allenic electronic structure of the azide ligand an angle of 90° would be expected. However, as indicated in Table VI the angle between planes defined by Ni–N(1)–N(2) and Ni'–N(3)–N(2) is only 38.4 (15)°.

The geometry of the nickel–azide ring is quite different from that for the only other molecular complex crystallographically found to have an end-to-end di-μ-azido bridge, $Cu_2(P(C_6H_5)_3)_4(N_3)_2$.[5] In this molecule all Cu–N distances were equivalent and the Cu–N–N angles of the bridging azides average to 122°. The dihedral angles between Cu–N–N planes for the Cu–N_3–Cu' bridged units are 103°, more closely reflecting the allenic nature of the N_3^- ligand than the value found in the present case. While the bridging N_3^- ligands in $[Ni_2(tren)_2(N_3)_2]^{2+}$ form a nearly perfect plane, the azide ligands in $Cu_2(P(C_6H_5)_3)_4(N_3)_2$ are crossed (I). It is of interest that, while the geometries of the metal–azide rings differ in the Cu and Ni complexes, the N–N distances remain the same (~1.17 Å) in both cases. The asymmetric, parallel bridge in the nickel(II) dimer probably results from a combination of electronic and steric effects. As can be seen from Figures 1 and 2, with respect to a side view of the bridging structure, the two azide groups are staggered.

Table V. Principal Interatomic Distances and Angles for $[Ni_2(tren)_2(N_3)_2](B(C_6H_5)_4)_2$

Distances, Å			
Ni–N(1)	2.069 (8)	N(4)–C(5)	1.488 (7)
Ni–N(3)'	2.195 (7)	C(1)–C(2)	1.505 (10)
Ni–N(4)	2.078 (6)	C(2)–N(5)	1.478 (9)
Ni–N(5)	2.079 (6)	C(3)–C(4)	1.536 (10)
Ni–N(6)	2.067 (5)	C(4)–N(6)	1.482 (9)
Ni–N(7)	2.117 (6)	C(5)–C(6)	1.516 (10)
N(1)–N(2)	1.173 (8)	C(6)–N(7)	1.485 (10)
N(2)–N(3)	1.174 (8)	C–H (av)	1.03 (3)
N(4)–C(1)	1.526 (7)	N–H (av)	0.99 (2)
N(4)–C(3)	1.519 (8)	Ni- - -Ni'	5.220 (2)
Angles, deg			
Ni–N(1)–N(2)	135.3 (7)	N(1)–N(2)–N(3)	177.1 (9)
Ni–N(3)'–N(2)'	123.3 (6)	N(4)–C(1)–C(2)	106.4 (6)
N(1)–Ni–N(3)'	91.7 (3)	C(1)–C(2)–N(5)	109.9 (6)
N(1)–Ni–N(4)	171.1 (2)	Ni–N(5)–C(2)	107.6 (4)
N(1)–Ni–N(5)	102.0 (3)	N(4)–C(3)–C(4)	112.2 (6)
N(1)–Ni–N(6)	89.5 (2)	C(3)–C(4)–N(6)	107.2 (6)
N(1)–Ni–N(7)	94.1 (3)	Ni–N(6)–C(4)	106.5 (4)
N(3)'–Ni–N(4)	95.3 (2)	N(4)–C(5)–C(6)	108.8 (6)
N(3)'–Ni–N(5)	87.2 (2)	C(5)–C(6)–N(7)	109.5 (6)
N(3)'–Ni–N(6)	178.6 (3)	Ni–N(7)–C(6)	111.3 (4)
N(3)'–Ni–N(7)	82.9 (2)	Ni–N(4)–C(1)	107.0 (4)
N(4)–Ni–N(5)	84.0 (2)	Ni–N(4)–C(3)	108.8 (4)
N(4)–Ni–N(6)	83.5 (2)	Ni–N(4)–C(5)	106.0 (4)
N(4)–Ni–N(7)	81.2 (2)	C(1)–N(4)–C(3)	111.0 (5)
N(5)–Ni–N(6)	93.4 (2)	C(1)–N(4)–C(5)	112.1 (5)
N(5)–Ni–N(7)	161.3 (3)	C(3)–N(4)–C(5)	111.6 (5)
N(6)–Ni–N(7)	96.2 (2)		

Table VI. Dihedral Angles and Least-Squares Planes for $[Ni(tren)N_3]_2(B(C_6H_5)_4)_2$

Dihedral Angles

Plane 1	Plane 2	Angle, deg
Ni, N(1), N(3)'	N(1), N(2)', N(3)	20.7 (4)
Ni, N(1), N(2)	Ni', N(2), N(3)	38.4 (15)

Least-Squares Planes[a]

Atom	Distance, Å	Atom	Distance, Å
Azide Plane[b] $6.31X - 4.62Y + 5.83Z = 0.00$			
Ni	0.52	N(7)	−1.46
N(1)	0.00	C(1)	2.19
N(2)	0.00	C(2)	3.14
N(3)	0.00	C(3)	1.10
N(4)	0.92	C(4)	0.55
N(5)	2.51	C(5)	−0.27
N(6)	1.00	C(6)	−1.52
Tetragonal Plane of the Complex[c] $3.08X - 9.23Y + 6.63Z = 0.27$			
Ni	0.004 (1)	N(7)	−1.463
N(1)	−0.123 (7)	C(1)	2.189
N(2)	0.224	C(2)	3.142
N(3)	0.575	C(3)	1.101
N(3)'	−0.025 (7)	C(4)	0.554
N(4)	−0.067 (5)	C(5)	−0.267
N(5)	2.058	C(6)	−1.522
N(6)	0.005 (6)		

[a] Least-squares planes calculated according to W. C. Hamilton, *Acta Crystallogr.*, 14, 185 (1961). Equations given in monoclinic coordinates. [b] Atoms included in calculation of the plane are N(1), N(2)', N(3). [c] Atoms included in calculation of the plane are Ni, N(1), N(3)', N(4), N(6).

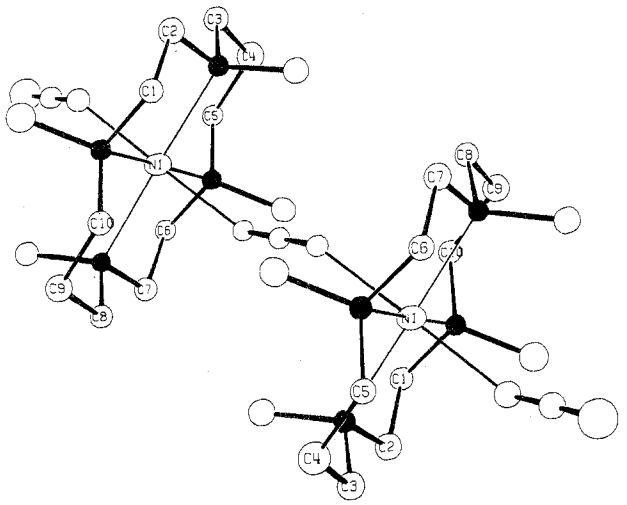

Figure 3. ORTEP plotting of $[Ni_2(macro)_2(N_3)_3]^+$; hydrogen atoms are not shown.

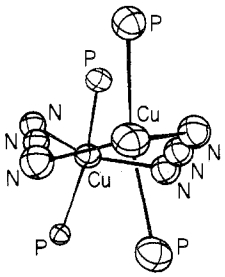

I

The eight-membered rings formed by bridging thiocyanate ligands in complexes of Ni and Cu which are related to the azide complexes above offer an interesting comparison. The $M_2(SCN)_2$ eight-membered rings of $Cu_2(P(C_6H_5)_3)_4(SCN)_2$ and the ferromagnetically coupled complex $[Ni_2(en)_4(SCN)_2]^{2+}$ are both essentially planar.[15,16] Bond angles to the metal at the sulfur are quite similar with values of 99 and 100° for Cu–S–C and Ni–S–C angles, respectively. The M–N–C and S–M–N angles differ somewhat in the two complexes with values of 167 and 100° for the Ni complex and 158 and 102° for $Cu_2(P(C_6H_5)_3)_4(SCN)_2$. Differences in the values of these angles probably reflect the change in coordination geometry. However, it is clear that the planar ring may result with bridging thiocyanate ligands without unusual deviation from normal coordination geometry.

The tren Ligand. Nitrogen donors of the chelating tren ligand occupy the remaining four positions about the octahedral Ni atom. Angles of the carbon atoms bonded to the tertiary tren nitrogen (N(4)) reflect a normal trigonal geometry. However, with the flexibility of the ethylene bridges, two nitrogens are bonded to the Ni in positions which are mutually trans (N(5) and N(7)) while the third (N(6)) occupies a position cis to the other tren nitrogens. Nickel–nitrogen distances are within the range of expected values (2.06–2.07 Å) for N(4), N(5), and N(6); N(7) is slightly out of position and has a longer value of 2.117 (6) Å. The normal trigonal geometry of the ligand seems to be responsible for displacement of N(7) toward the N(4)–Ni–N(3)' plane with N(7)–Ni–N(4) and N(7)–Ni–N(3)' angles of 81.2 (2) and 82.9 (2)°, respectively, and an N(7)–Ni–N(5) angle of 161.3 (3)°.

Susceptibility Results and Discussion

The variable-temperature magnetic susceptibility data for $[Ni_2(tren)_2(N_3)_2](BPh_4)_2$ have been analyzed[6] in terms of the theoretical equations for a nickel(II) dimer as put forth by Ginsberg, *et al.*[17] There is a relatively strong antiferromagnetic interaction characterized by an *intra*dimer isotropic exchange parameter J of -35.1 cm^{-1}, a g value of 2.325, a single-ion zero-field parameter D of 6.8 cm^{-1}, and an effective *inter*dimer exchange $Z'J'$ of 0.50°. A qualitative discussion of the exchange mechanism operative in this compound has also been presented.[6]

In light of the above work, it was of considerable interest that a compound possessing a *single* 1,3-μ-azido bridge was isolated by two of the present authors and characterized by X-ray work.[7] As part of a study of the nitrogen configurations in metal complexes of tetra-*N*-methyl macrocyclic ligands, it was found that the cation in $[Ni_2(macro)_2(N_3)_3]I$ has the structure depicted in Figure 3. This is the only dimeric complex with a *single* end-to-end azide bridge that has been authenticated by X-ray work. Single azido bridging has been

Table VII. Experimental and Calculated Magnetic Susceptibility Data for $[Ni_2(macro)_2(N_3)_3]I$[a]

	$10^3\chi_M$, cgsu		μ_{eff}/Ni, BM	
T, °K	Obsd	Calcd	Obsd	Calcd
296.1	7.45	8.07	2.971	3.090
230.3	9.62	10.11	2.977	3.052
161.0	13.42	13.82	2.940	2.983
97.7	20.84	20.72	2.853	2.846
58.0	29.46	29.46	2.614	2.614
46.5	32.94	33.00	2.475	2.477
39.1	35.36	35.36	2.251	2.251
32.6	37.30	37.17	2.205	2.201
24.1	27.76	38.16	1.908	1.918
19.2	36.06	37.05	1.664	1.687
14.4	33.43	33.56	1.387	1.390
10.7	28.65	27.48	1.107	1.084
8.2	20.96	19.86	0.829	0.807
6.6	13.17	13.04	0.589	0.587
5.4	6.39	7.60	0.371	0.405
4.8	4.10	5.17	0.280	0.315
4.2	2.53	3.18	0.206	0.231

[a] Diamagnetic correction used: -552.0×10^{-6} cgsu/mol. Theoretical parameters: $J = -12.3$ cm^{-1}, $g = 2.233$, $D = 4.9$ cm^{-1}, $Z'J' = -1.2°$. Standard error SE = 0.045 where SE = $\{\Sigma_{i=1}^{n}[\mu_{eff}(obsd)_i - \mu_{eff}(calcd)_i]^2/(n-K)\}^{1/2}$ and K is the number of parameters used to fit the n data points.

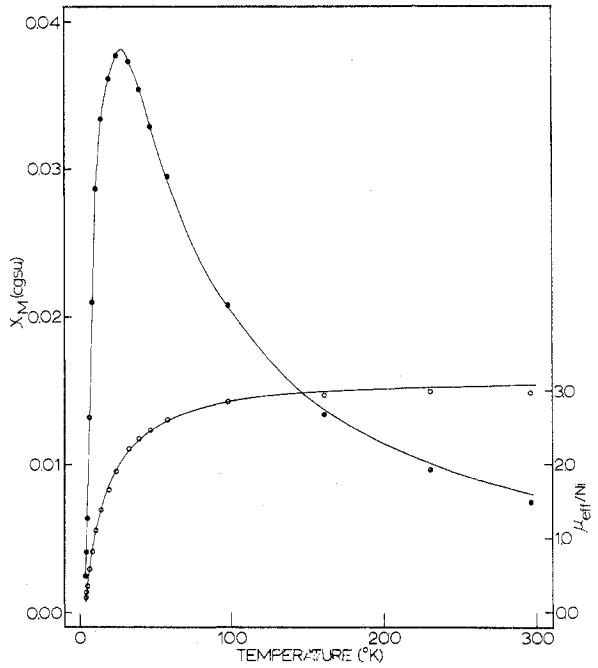

Figure 4. Molar paramagnetic susceptibility (cgsu/mol) and effective magnetic moment per nickel (BM/nickel) curves for $[Ni_2(macro)_2(N_3)_3]I$ in a magnetic field of 14.8 kG. The circles are experimental data, whereas the lines are least-squares fit using a theoretical expression (see text).

Table VIII. Nonvirtual CNDO/2 Molecular Orbitals and Eigenvalues for $H_2N_3^+$ with Three Different Dihedral Angles

0° Dihedral Angle[a]

	Symmetry							
	$1a_g$	$1b_u$	$2a_g$	$2b_u$	$1a_u$	$3b_u$	$3a_g$	$1b_g$
	Eigenvalues, eV							
	−2.0897	−1.8259	−1.3514	−1.3145	−1.2512	−1.1421	−0.9494	−0.8379
H(1) s	−0.1512	−0.2256	0.3355	0.2866	−0.0000	0.1467	−0.2569	0.0000
N(1) s	−0.4149	−0.5269	0.3861	−0.0269	0.0000	0.2803	0.2715	0.0000
N(1) p_x	0.0223	0.0564	−0.1423	−0.4511	0.0000	0.1797	0.5841	0.0000
N(1) p_y	−0.0000	−0.0000	0.0000	−0.0000	0.4865	0.0000	0.0000	−0.7071
N(1) p_z	−0.1952	−0.0860	−0.3805	−0.1933	−0.0000	−0.4560	−0.1171	−0.0000
N(2) s	−0.7299	0.0000	−0.3830	0.0000	−0.0000	0.0000	−0.1040	−0.0000
N(2) p_x	0.0000	0.0512	−0.0000	0.5346	0.0000	0.3642	−0.0000	0.0000
N(2) p_y	−0.0000	−0.0000	−0.0000	0.0000	0.7257	−0.0000	−0.0000	0.0000
N(2) p_z	0.0000	0.5651	0.0000	0.2582	−0.0000	0.4322	−0.0000	0.0000
N(3) s	−0.4149	0.5269	0.3861	0.0269	0.0000	−0.2803	0.2715	0.0000
N(3) p_x	−0.0223	0.0564	0.1423	−0.4511	−0.0000	0.1797	−0.5841	0.0000
N(3) p_y	−0.0000	0.0000	−0.0000	0.0000	0.4865	−0.0000	0.0000	0.7071
N(3) p_z	0.1952	−0.0860	0.3805	−0.1933	0.0000	−0.4560	0.1171	−0.0000
H(2) s	−0.1512	0.2256	0.3355	−0.2866	0.0000	−0.1467	−0.2569	−0.0000

90° Dihedral Angle[b]

	Symmetry							
	1a	1b	2a	2b	3a	3b	4a	4b
	Eigenvalues, eV							
	−2.0744	−1.8226	−1.3833	−1.2988	−1.2404	−1.1609	−0.9247	−0.9224
H(1) s	0.1585	0.2272	0.3410	−0.2730	0.0288	0.1507	0.2221	−0.2071
N(1) s	0.4327	0.5431	0.3062	0.0142	−0.2813	0.2390	−0.1715	0.1640
N(1) p_x	0.0037	−0.0067	0.0899	0.2117	0.2525	0.1731	−0.4168	−0.4151
N(1) p_y	0.0262	0.0481	0.2418	−0.4028	0.3515	−0.1311	0.4085	−0.4108
N(1) p_z	0.1959	0.0786	−0.3549	0.2068	0.2174	−0.4652	0.0694	−0.1319
N(2) s	0.7050	−0.0000	−0.3565	0.0000	0.1702	0.0000	0.0543	0.0000
N(2) p_x	0.0106	−0.0244	0.1841	0.3786	0.4135	0.2591	−0.2727	−0.2621
N(2) p_y	0.0106	0.0244	0.1841	−0.3786	0.4135	−0.2591	−0.2727	0.2621
N(2) p_z	−0.0000	−0.5373	−0.0000	−0.2534	−0.0000	0.4230	−0.0000	0.0783
N(3) s	0.4327	−0.5431	0.3062	−0.0142	−0.2813	−0.2390	−0.1715	−0.1640
N(3) p_x	0.0262	−0.0481	0.2418	0.4028	0.3513	0.1311	0.4085	0.4108
N(3) p_y	0.0037	0.0067	0.0899	−0.2117	0.2525	−0.1731	−0.4168	0.4151
N(3) p_z	−0.1959	0.0786	0.3549	0.2068	−0.2174	−0.4652	−0.0694	−0.1319
H(2) s	0.1585	−0.2272	0.3410	0.2730	0.0288	−0.1507	0.2221	0.2071

38.4° Dihedral Angle[c]

	Symmetry							
	1a	1b	2a	2b	3a	3b	4a	4b
	Eigenvalues, eV							
	−2.0762	−1.8201	−1.3934	−1.2626	−1.2391	−1.1819	−0.9550	−0.8717
H(1) s	0.1593	0.2254	−0.3486	0.2406	−0.0160	−0.2067	0.2195	−0.1686
N(1) s	0.4286	0.5408	−0.2732	0.0200	0.3319	−0.1939	−0.2244	0.1033
N(1) p_x	0.0048	0.0013	−0.0501	−0.3428	−0.0791	−0.2551	0.1963	0.5752
N(1) p_y	0.0296	0.0434	−0.2938	0.2997	−0.3900	−0.0127	0.5237	−0.2464
N(1) p_z	0.1954	0.0806	0.3286	−0.2076	−0.2542	0.4366	0.1995	−0.0352
N(2) s	0.7094	−0.0001	0.3404	0.0000	−0.2036	−0.0001	0.0000	−0.0283
N(2) p_x	0.0072	−0.0129	−0.1032	−0.5391	−0.1776	−0.3663	0.2694	0.1211
N(2) p_y	0.0207	0.0045	−0.2963	0.1876	−0.5102	0.1276	−0.0939	0.3475
N(2) p_z	−0.0000	−0.5445	−0.0002	0.2380	0.0000	−0.4207	−0.1276	0.0000
N(3) s	0.4285	−0.5408	−0.2733	−0.0201	0.3319	0.1941	0.2243	0.1033
N(3) p_x	0.0146	−0.0259	−0.1432	−0.4549	−0.1802	−0.1920	−0.1715	−0.6038
N(3) p_y	0.0262	−0.0348	−0.2613	−0.0220	−0.3548	0.1685	−0.5323	0.1643
N(3) p_z	−0.1954	0.0807	−0.3284	−0.2076	0.2541	0.4367	0.1995	0.0352
H(2) s	0.1592	−0.2253	−0.3484	−0.2407	−0.0160	0.2068	−0.2196	−0.1687

[a] Atomic coordinates (x, y, z): H(1) (−0.888, 0.0, −1.633); N(1) (0.0, 0.0, −1.235); N(2) (0.0, 0.0, 0.0); N(3) (0.0, 0.0, 1.235); H(2) (0.888, 0.0, 1.633). [b] Atomic coordinates (x, y, z): H(1) (0.0, 0.888, −1.633); N(1) (0.0, 0.0, −1.235); N(2) (0.0, 0.0, 0.0); N(3) (0.0, 0.0, 1.235); H(2) (0.888, 0.0, 1.633). [c] Atomic coordinates (x, y, z): H(1) (0.0, 0.888, −1.633); N(1) (0.0, 0.0, −1.235); N(2) (0.0, 0.0, 0.0); N(3) (0.0, 0.0, 1.235); H(2) (0.552, 0.696, 1.633).

claimed for $M_2(PPh_3)_4(CO)_2N_3^+$, M = Rh, Ir,[18] and for a solid[19] which contained two molecules of tetraphenylporphineiron(III) azide per molecule of tetraphenylporphineiron(III): X-ray work[20] on $Mn(acac)_2N_3$ shows that the azide group bridges adjacent Mn(III) atoms to form polymeric chains of six-coordinate Mn(III) polyhedra.

The magnetic susceptibility of $[Ni_2(macro)_2(N_3)_3]I$ was measured throughout the temperature range of 4.2–296°K and the results are given in Table VII and are illustrated in Figure 4. The susceptibility increases with decreasing temperature until a maximum is reached at 25°K; at lower temperatures the susceptibility decreases rapidly. In the case of both the paramagnetic susceptibility (χ) *vs.* temperature and the effective magnetic moment per nickel(II) (μ_{eff}/Ni) *vs.* temperature curves, the points represent the experimental data, whereas the solid lines are theoretical lines least-squares fit to the nickel dimer equation.[17] This gives $J = -12.3$ cm^{-1}, $g = 2.233$, $D = 4.9$ cm^{-1}, and $Z'J' = -1.2°$. Thus, the singly azide-bridged system has a considerably weaker antiferromagnetic exchange interaction than was found for $[Ni_2(tren)_2(N_3)_2](BPh_4)_2$ and it is here, then, that we turn to a qualitative description of the factors that are determining this difference in exchange interaction.

A list of the important factors leading to the above difference in exchange interaction would contain (1) the greater potential for exchange of two bridges *vs.* a single bridge, (2) the differences in bridging geometries, and (3) any possible differences in electronic states at the nickel centers in the two dimers. In the case of this last factor we are concerned with whether the unpaired electron density at the metal ions of $[Ni_2(tren)_2(N_3)_2](BPh_4)_2$ has a different orientation with respect to the bridging azides than is present in $[Ni_2(macro)_2(N_3)_3]I$. This is difficult to determine and perhaps all that can be said at this time is that one usually assumes such nickel(II) centers are magnetically isotropic (*i.e.*, $g_{zz} = g_{yy} = g_{xx}$).

It can be shown[21] for a system of two electrons, each on separate nuclear centers, that, employing a Hamiltonian operator with kinetic and potential (electron–electron and electron–nuclear) energy terms, the energy separation between the singlet (paired electrons) electronic state of this two-electron system and the triplet (unpaired electrons) state is a function of exchange, Coulomb, and overlap integrals. If we relate this to the effective Hamiltonian $H = -2JS_i \cdot S_j$, the exchange parameter J is likewise a function of exchange, Coulomb, and overlap integrals. These integrals are to be evaluated over molecular orbitals, which are composed of atomic orbitals. If everything else is equivalent, the di-μ-azido-bridged dimer would be expected to have a larger $|J|$ than the mono-μ-azido-bridged dimer. The reduction in net antiferromagnetic interaction in going from the dibridged ($J = -35$ cm^{-1}) to the monobridged ($J = -12$ cm^{-1}) systems is probably largely due to this factor. The decrease in $|J|$ seems, however, to be greater than would be expected, and thus we turn to an appraisal of the influence of any differences in bridging geometries.

In reference to Figure 3, the cation in $[Ni_2(macro)_2(N_3)_3]I$ has a crystallographic center of symmetry coincident with the central nitrogen atom of the bridging azide ion. The bridging azide N–N distance is found to be 1.17 (1) Å which is equivalent to the mean value for $[Ni_2(tren)_2(N_3)_2](BPh_4)_2$. The Ni–N (bridge azide) distance is 2.15 (1) Å which is to be compared with the dibridged compound's distances of Ni–N(3)′ = 2.195 (7) Å and Ni–N(1) = 2.069 (8) Å. In both cases the bridging azides are linear. An interesting comparison is found in the Ni–N–N angles. Empirically, it has been found[4] that azide generally binds to a metal such that this angle approaches 120°. As we already noted, the two Ni–N–N angles in $[Ni_2(tren)_2(N_3)_2](BPh_4)_2$ are 135.3 (7) and 123.3 (6)°. The Ni–N–N angle in the singly bridged compound is 142°, possibly a reflection of steric considerations in the solid state. The most interesting difference between the two structures is in dihedral angles between the planes defined by each nickel and its two nearest azide nitrogen atoms. In the di-μ-azide compound this angle is 38.4°, whereas in the mono-μ-azide compound (see Figure 3) this angle is 0°.

The above differences in bridging geometries could also explain, in part, the weaker antiferromagnetic interaction in the mono-μ-azide compound relative to that found for the di-μ-azide compound. For instance, if 120° is the optimal bonding angle for N_3^- bonding to a metal, then the larger angle of 142° in $[Ni_2(macro)_2(N_3)_3]I$ could point to a decreased metal–azide overlap relative to the di-μ-azide case.

A weaker antiferromagnetic interaction in $[Ni_2(macro)_2(N_3)_3]I$ could also result from the 0° dihedral angle. It is not possible to check this quantitatively; however, a qualitative analysis based largely on symmetry considerations can be presented. If the Ni–N_3–Ni unit possesses a dihedral angle of 0° with the trans configuration, the bridging unit belongs to the C_{2h} point group. The unpaired electrons are in molecular orbitals that are probably dominantly metal $3d_{x^2-y^2}$ and $3d_{z^2}$ in character and these four orbitals (two on each nickel center) form a representation that contains only a_g and b_u irreducible representations. These four metal d orbitals will interact with azide orbitals of the correct symmetry and thereby provide potential "pathways"[21] for antiferromagnetic exchange between the two nickel centers. If the Ni–N_3–Ni plane is defined to be the xz plane, then the nitrogen $2p_y$ orbitals form representations of a_u and b_g symmetry and are thus not involved in exchange pathways. When the dihedral angle is different from 0°, then the symmetry of the Ni–N_3–Ni unit is reduced to C_2 and *all* orbitals are of either a or b symmetry. Since the four "magnetic" nickel orbitals form a representation in C_2 that is reducible to two a and two b irreducible representations, all azide bridge orbitals are of a symmetry admitting of metal–bridge overlap and thus are potential exchange pathways.

It may at this point be suggested that since the bridging symmetry in $[Ni_2(macro)_2(N_3)_3]I$ is C_{2h} (dihedral angle 0°) whereas that for the $Ni_2(tren)_2(N_3)_2^{2+}$ ion is C_2 (dihedral angle 38.4°), then the larger number of *potential* pathways for the latter compound results in a greater antiferromagnetic exchange. However, it is the *viability* (*i.e.*, the atomic orbital composition) of each of these pathways that determines the exchange parameter and not primarily the number of pathways. It would be desirable to have molecular orbital calculations on these metal-containing dimers, but this is not practical and as such we turn to CNDO/2 calculations on $H_2N_3^+$ to illustrate the variation of molecular orbital composition as a function of dihedral angle.

Molecular orbital calculations were performed on H–N_3–H^+ with an N–H bond length of 0.97 Å, with an N–N bond length of 1.235 Å (these dimensions were selected from a previous[22] MO calculation of N_3^- and HN_3), and with the three dihedral angles of 0, 38.4, and 90°. It is instructive to look first at the filled molecular orbitals obtained for the two limiting cases of 0 and 90°; these are given in Table VIII. The symmetries of the various orbitals for the 0° case are given, and as can be seen by the coefficients, only those of a_g or b_u character are appropriate for N–H bonding interactions, which is consistent with the previous discussion of nickel–azide bonding requirements. One of the six a_g and b_u symmetry orbitals, the $3a_g$ orbital, is not a viable pathway for exchange interaction because the central nitrogen atom has only 2s character which is antibonding with respect to the 2s character on the terminal azide nitrogen atoms. The other five a_g and b_u orbitals are bonding between the two hydrogens through either the σ (p_z and s) orbitals of the bridge or the in-(xz) plane "π orbitals."

The $1a_g$, $1b_u$, $3b_u$, and $2a_g$ orbitals are purely σ in nature, whereas the $2b_u$ is both a σ and an in-plane π pathway.

When the dihedral angle is changed to 90°, keeping *everything else constant*, bonding between the hydrogen atoms and the azide is found in all eight molecular orbitals, as expected; however, only five orbitals are found with bonding overlaps between the two hydrogens. These are the 1a, 1b, 2a, 2b, and 3b orbitals, which are, of course, the analogs of the $1a_g$, $1b_u$, $2a_g$, $2b_u$, and $3b_u$ orbitals for the 0° case; the σ overlaps should not change as a function of the dihedral angle. In the 90° case no in-plane π bonding is possible due to the noncoplanarity of the hydrogen atoms.

Thus, it appears that even though for the 90° case the hydrogens bond into both p_x and p_y orbitals on the azide terminal nitrogen atoms, whereas this is more restricted for the 0° case, zero overlap between the p_x and p_y systems eliminates any exchange possibilities through these orbitals. On the basis of this simple analysis antiferromagnetic exchange through the 90° system would *not* be greater than through the 0° system and it might be less.

However, the dihedral angle for the bridges in $Ni_2(tren)_2(N_3)_2^{2+}$ is 38.4°, and for this intermediate case nitrogen atom p_x and p_y admixture results in net bonding interactions (*via* the N_3^- bridges) between the two metals in orbitals that in the 0 and 90° cases are *not* viable antiferromagnetic exchange pathways. These interactions may well account, in part, for the increased antiferromagnetic exchange in $[Ni_2(tren)_2(N_3)_2](BPh_4)_2$ compared to $[Ni_2(macro)_2(N_3)_3]I$. A CNDO/2 calculation for $H_2N_3^+$ with a 38.4° dihedral angle gives the molecular orbitals as listed in Table VIII. Inspection of the composition of the orbitals for this case shows the admixture of p_x and p_y in several orbitals. It is realized that these "model" calculations cannot represent all aspects of the metal-containing systems but can be taken to suggest the possible dependence of exchange on the dihedral angle.

Acknowledgment. We are very grateful for support from National Institutes of Health Grant HL 13652 (D.N.H.) and the National Science Foundation (E.K.B.).

Registry No. $[Ni_2(tren)_2(N_3)_2](BPh_4)_2$, 53730-64-6; $[Ni_2(macro)_2(N_3)_3]I$, 52588-40-6.

Supplementary Material Available. The final values of $|F_o|$ and $|F_c|$ for 1982 reflections will appear following these pages in the microfilm edition of this volume of the journal. Photocopies of the supplementary material from this paper only or microfiche (105 × 148 mm, 24× reduction, negatives) containing all of the supplementary material for the papers in this issue may be obtained from the Journals Department, American Chemical Society, 1155 16th St., N.W. Washington, D.C. 20036. Remit check or money order for $3.00 for photocopy or $2.00 for microfiche, referring to code number AIC40353L.

References and Notes

(1) West Virginia University.
(2) University of Illinois.
(3) Camille and Henry Dreyfus Fellow, 1972–1977.
(4) Z. Dori and R. F. Ziolo, *Chem. Rev.*, **73**, 247 (1973).
(5) R. F. Ziolo, A. P. Gaughan, Z. Dori, C. G. Pierpont, and R. Eisenberg, *Inorg. Chem.*, **10**, 1289 (1971).
(6) D. M. Duggan and D. N. Hendrickson, *Inorg. Chem.*, **12**, 2422 (1973).
(7) F. Wagner, M. T. Mocella, M. J. D'Aniello, Jr., A. H.-J. Wang, and E. K. Barefield, *J. Amer. Chem. Soc.*, **96**, 2625 (1974).
(8) D. M. Duggan, E. K. Barefield, and D. N. Hendrickson, *Inorg. Chem.*, **12**, 985 (1973).
(9) T. C. Furnas, "Single Crystal Orienter Instruction Manual," General Electric Co., Milwaukee, Wis., 1957, Chapter 10.
(10) J. Reed, A. J. Schultz, C. G. Pierpont, and R. Eisenberg, *Inorg. Chem.*, **12**, 2949 (1973).
(11) D. T. Cromer and J. T. Waber, *Acta Crystallogr.*, **18**, 104 (1965).
(12) R. F. Stewart, E. R. Davidson, and W. T. Simpson, *J. Chem. Phys.*, **42**, 3175 (1965).
(13) D. T. Cromer and D. Liberman, *J. Chem. Phys.*, **53**, 1891 (1970).
(14) See paragraph at end of paper regarding supplementary material.
(15) A. P. Gaughan, R. F. Ziolo, and Z. Dori, *Inorg. Chim. Acta*, **4**, 640 (1970).
(16) A. E. Shvelashvili, M. A. Porai-Koshits, and A. S. Antsyshkina, *J. Struct. Chem. (USSR)*, **10**, 552 (1969).
(17) A. P. Ginsberg, R. L. Martin, R. W. Brookes, and R. C. Sherwood, *Inorg. Chem.*, **11**, 2884 (1972).
(18) K. V. Werner and W. Beck, *Chem. Ber.*, **105**, 3209 (1972).
(19) I. A. Cohen, *Ann. N.Y. Acad. Sci.*, **206**, 453 (1973).
(20) V. W. Day, B. R. Stults, E. L. Tasset, R. O. Day, and R. S. Marianelli, *J. Amer. Chem. Soc.*, **96**, 2650 (1974).
(21) A. P. Ginsberg, *Inorg. Chim. Acta, Rev.*, **5**, 45 (1971).
(22) R. Bonaccorsi, C. Petrongolo, E. Scrocco, and J. Tomasi, *J. Chem. Phys.*, **48**, 1500 (1968).